

Structure determination of oxygen adsorbates on Cu surfaces by means of the SEELFS technique

This article has been downloaded from IOPscience. Please scroll down to see the full text article.

1991 J. Phys.: Condens. Matter 3 2873

(<http://iopscience.iop.org/0953-8984/3/17/005>)

View [the table of contents for this issue](#), or go to the [journal homepage](#) for more

Download details:

IP Address: 171.66.16.147

The article was downloaded on 11/05/2010 at 12:04

Please note that [terms and conditions apply](#).

Structure determination of oxygen adsorbates on Cu surfaces by means of the SEELFS technique

B Luo and J Urban

Fritz-Haber-Institut der Max-Planck-Gesellschaft, Abteilung Elektronenmikroskopie, Faradayweg 4–6, 1000 Berlin 33, Federal Republic of Germany

Received 11 June 1990, in final form 17 October 1990

Abstract. The oxygen adsorption on Cu(110) and Cu(111) surfaces was studied by means of the SEELFS technique above the oxygen K-edge. The calculated partial cross sections show that the non-dipole transitions are much weaker than the dipole transitions. The phaseshift for the nearest-neighbour distance calculated by using the curved-wave approximation agrees with the reference phaseshift even though the plane-wave phaseshift deviates from it, hence the curved-wave approximation was applied to interpret the SEELFS data. A nearest-neighbour distance of 1.82 Å for the O/Cu(110) system and 1.91 Å for the O/Cu(111) system were obtained. The missing-row model of the (2×1) substructure of O/Cu(110) is a suitable one. In the O/Cu(111) system, the oxygen atoms are located about 0.5 Å above the topmost Cu layer.

1. Introduction

The SEXAFS technique (surface extended x-ray absorption fine structure) has become a powerful method for the determination of the geometrical structure in the vicinity of adsorbed atoms [1–6]. The O/Cu(110) and O/Cu(111) systems were investigated by Döbler *et al* [5], Haase *et al* [6–8, 46] and Bader *et al* [9] who used the SEXAFS technique. The neighbour distances were determined with high precision by means of the Fourier transform [10]. Reference phaseshifts obtained from experiments on model compounds (e.g. Cu₂O, CuO) [4] were used [5–8]. The reason for using actual reference phaseshifts lies in the fact that phaseshifts which are calculated by using the plane-wave approximation led to too short neighbour distances between adsorbates and substrates [11, 12]. An apparent shorter nearest-neighbour distance was also observed with the SEELFS (surface extended electron energy loss fine structure) and EXAFS studies above M_{2,3} edges of 3d transition elements provided the plane-wave phaseshifts were used for the data analysis [13–18]. An accurate interpretation of the SEELFS spectra is only possible with the curved-wave formalism [18, 19]. In the present work, we studied again the O/Cu systems, but used the SEELFS technique instead of the SEXAFS technique. The same technique has been applied by various authors [20–24] who studied other adsorbate structures. For the analysis of the SEELFS data, the curved-wave approximation [25–27] was used. To study a possible influence of the non-dipole transitions on the fine structure the partial cross sections for the oxygen K-edge were calculated by means of the Bethe formalism [28].

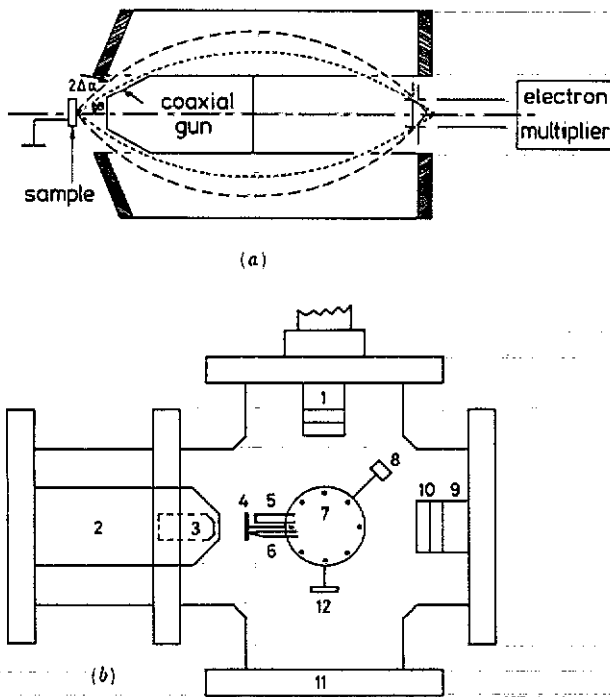


Figure 1. (a) The cylindrical mirror analyser. (b) The schematic diagram of the vacuum chamber: (1) ion gun; (2) CMA; (3) electron gun; (4) sample; (5) sample heater; (6) thermocouple; (7) sample holder; (8) Faraday cup; (9) evaporator; (10) mass spectrometer (quadrupole); (11) window; (12) microbalance.

2. Experiment

The Cu(110) and Cu(111) crystal surfaces were cleaned according to UHV standards [29]. The mechanically and chemically cleaned samples were bombarded by Ar ions at an Ar partial press of $1 \sim 3 \times 10^{-5}$ mbar. They were then annealed at $T = 400^\circ\text{C}$ for half an hour. The clean Cu(110) surface was exposed to a 2×10^{-5} mbar oxygen atmosphere for 5 minutes (600 L) and the Cu(111) surface for 10 minutes (1200 L). The contamination—mainly due to carbon—was continuously measured by Auger spectroscopy. Our UHV conditions ($\sim 10^{-11}$ mbar) ensured minimal contamination of the surface.

The SEELFS experiments were performed with a commercial Auger spectrometer in the reflection mode [13–15] (figure 1). The energy analyser was an OPC 105 CMA (cylindrical mirror analyser, Ribier) with a resolution of 0.5% and a transmission of 10%. The electron gun was positioned coaxially with respect to the CMA and the incident electron beam of $15 \mu\text{A}$ and 0.1 mm diameter was normal to the sample surface. The angle between the normal of the sample surface and the direction of the scattered electron is 42.5° .

The registration of the SEELFS data was carried out with a lock-in amplifier in the first derivative mode. A 6 V peak-to-peak modulation was used and the primary energy was 2000 eV.

The SEELFS spectrum for O/Cu(110) was obtained by averaging two measured spectra, which were obtained during less than 30 minutes, respectively. Further

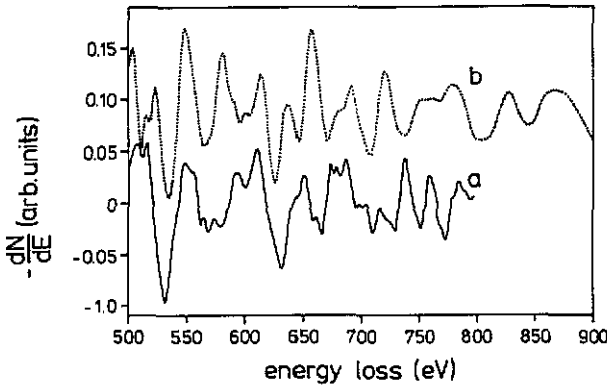


Figure 2. The SEELFS spectra of the oxygen K-edge. The primary energy was 2000 eV. These spectra were obtained after background subtraction. a: O/Cu(110); b: O/Cu(111).

measurements introduced some changes of the SEELFS spectra. The SEELFS spectrum for O/Cu(111) which was obtained during 15 minutes has been smoothed. The SEELFS signal for this system disappeared after this measurement. The spectra after fitting the background by spline functions are shown in figure 2. They were then transformed into k -space by means of the following relation [30]:

$$k = \frac{\sqrt{2m}}{\hbar} \sqrt{\Delta E - E_0} \quad (1)$$

where ΔE is the energy loss and E_0 the binding energy. Before performing the Fourier transform, the spectra were integrated.

3. Interpretation

The analysis of the SEELFS spectra is based on the curved-wave approximation. According to Müller and Schaich [25] and McKale *et al* [26], the SEELFS signal $\chi^1(k)$ of an $l = 1$ final state is given by [19]:

$$\chi^1(k) = \sum_j -3 \cos \theta_j^2 |\bar{f}_1(\pi, k, R_j)| \frac{N_j}{kR_j^2} e^{-2\sigma_j^2 k^2} e^{-2R_j/\lambda(k)} \sin(2kR_j + 2\delta_1 + \varphi_1(k, R_j)). \quad (2)$$

$\bar{f}_1(\pi, k, R_j)$ is the backscattering amplitude:

$$\bar{f}_1(\pi, k, R_j) = |\bar{f}_1(\pi, k, R_j)| e^{i\varphi_1(k, R_j)} = \frac{1}{k} \sum_{l'} (2l' + 1) (-1)^{l'} e^{i\delta_{l'}} \sin \delta_{l'} H(1, l', kR_j) \quad (3)$$

with

$$H(1, l', kR_j) = \sum_{\bar{l}} (2\bar{l} + 1) \left(\begin{pmatrix} 1 & l' & \bar{l} \\ 0 & 0 & 0 \end{pmatrix} h_{\bar{l}}^{(1)}(kR_j) \right)^2 (-1)^{\bar{l}} (kR_j)^2 e^{-i2kR_j}$$

where k is the wave vector, R_j the neighbour distance of the j atoms with a coordination

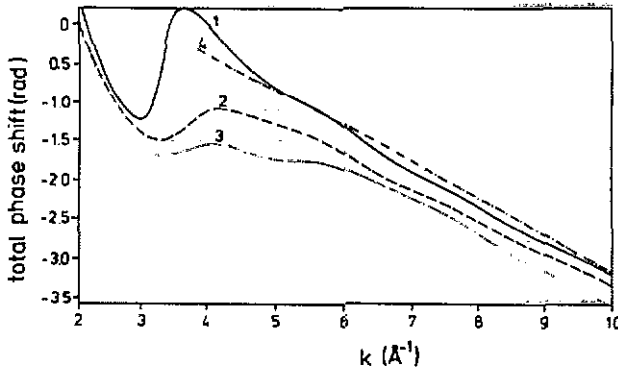


Figure 3. Total phaseshifts of the O-Cu system, O as central atom and Cu as backscatterer: (1) calculated by using the curved-wave approximation for $l = 1$ final state, $R = 2.0 \text{ \AA}$; (2) calculated by using the curved-wave approximation for $l = 1$ final state, $R = 3.1 \text{ \AA}$; (3) calculated by using the plane-wave approximation for $l = 1$ final state; (4) reference phase-shift taken from experimental data of Cu_2O [4].

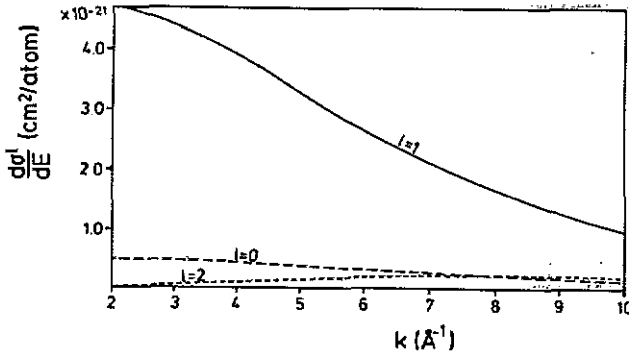


Figure 4. The differential partial cross sections of the oxygen K-edge for the primary energy of 2000 eV.

number of N_j . $|\tilde{f}_j(\pi, k, R_j)|$ and $\varphi_j(k, R_j)$ are the backscattering amplitude and the backscattering phaseshift of the j atoms, respectively. σ_j^2 is the Debye-Waller factor which describes the thermal disorder effects. $\lambda(k)$ is the mean free path of the excited electrons and δ_l the central phase shift. $h_j^{(1)}$ is the spherical Hankel function [31] and

$$\begin{pmatrix} 1 & l' & \bar{l} \\ 0 & 0 & 0 \end{pmatrix}$$

the $3j$ Wigner symbol [32]. $\delta_{l'}$ is the phaseshift of the backscattered l' partial wave. $3 \cos \theta_j^2$ is the polarization factor, where θ_j is the angle between R_j and the momentum transfer. In the case of the SEELFS technique, the two-step process—an inelastic process, followed or preceded by an elastic process—is more preferred than the single inelastic process [13, 19]. One can assume approximately that the effective incident electron beam (cf such electrons which only undergo one or more elastic processes) distributes spherical symmetrically. Then the polarization factor is nearly unity. It means that under

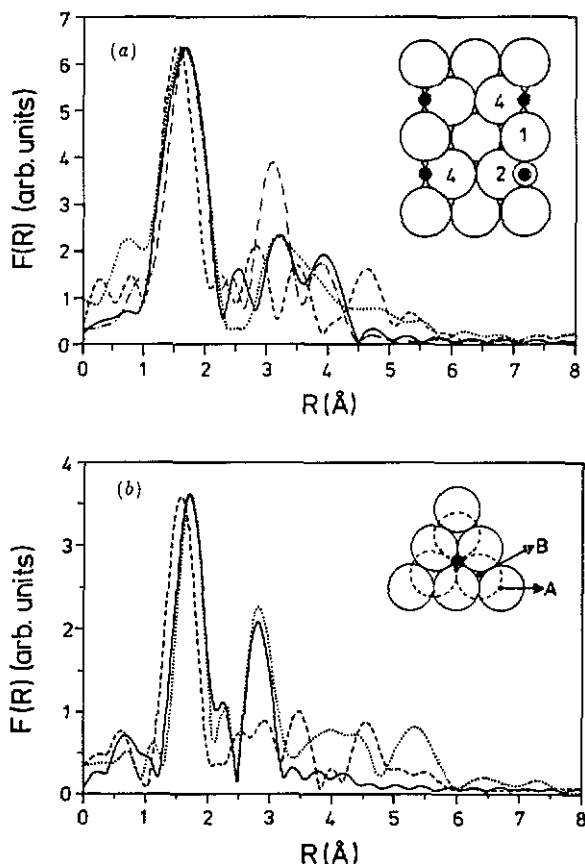


Figure 5. (a) The Fourier transforms of the O/Cu(110) system. The integration range was $2.0 < k < 8.0 \text{ \AA}^{-1}$. Dotted curve, measured Fourier transform; full curve, curved-wave Fourier transform of the missing-row model with the following neighbour atoms: copper atoms at 1.82, 1.97, 3.21 and 4.11 \AA and two oxygen atoms at 3.62 \AA (this missing-row model is shown in the inset); chain curve, curved-wave Fourier transform of the buckled (2×1) model [9]; broken curve, Fourier transform of Cu_2O . (b) The Fourier transforms of the O/Cu(111) system. The integration range was $2.0 < k < 9.3 \text{ \AA}^{-1}$. Dotted curve, measured Fourier transform; full curve, curved-wave Fourier transform for the copper neighbour atoms with $R_1 = 1.91$, $R_2 = R_3 = 2.98 \text{ \AA}$ (the atomic arrangement is shown in the inset) and three oxygen atoms at $R = 2.56 \text{ \AA}$; broken curve, Fourier transform of Cu_2O .

our experimental conditions all neighbour atoms (independent of their orientation) contribute to the SEELFS signal with the same amplitude.

The phaseshifts δ_l of a copper and oxygen backscatter were calculated by using the Hartree-Fock-Slater equation [33]. The backscattering amplitudes and phaseshifts were calculated for the $l = 1$ dipole transition and for the distances of 2.0 and 3.1 \AA according to (2). The central phaseshifts of oxygen from Teo and Lee [34] were used. The total phaseshifts—calculated by using the curved-wave approximation—are shown in figure 3. They are compared with the plane-wave total phaseshifts of the $l = 1$ contribution and with the experimental total phaseshifts of Cu_2O [4].

In order to control the deviation of the partial cross sections of the oxygen K-edge from the dipole approximation the partial differential cross sections were calculated by

means of the method of Cooper and Manson [35–37]. The results are shown in figure 4. The non-dipole transitions are very weak in comparison to the dipole transition, but there exist strong non-dipole transitions for some shallow edges (e.g. Cu $M_{2,3}$ [19] and Pd $N_{2,3}$ [38]), the reason being that the value of $qr - q$ is the momentum transfer and r the position vector of the electrons in the target atom—is much smaller for a K-edge of oxygen than for some shallow edges [21]. Therefore, in the case of the oxygen K-edge it is only necessary to consider the dipole transition.

According to LEED studies [39, 40], the oxygen atoms—adsorbed on the Cu(110) surface—form a (2×1) substructure after 600 L exposure. Hence, by using the missing-row (2×1) substructure model [9] with the copper neighbour atoms in the first layer (1.82 Å), in the second layer (1.97 Å and 4.11 Å) and in the third layer (3.21 Å) and the two oxygen atoms at 3.62 Å (figure 5(a)), a SEELFS spectrum was calculated by means of (2). Further model calculations were performed by using the buckled (2×1) model and for the Cu_2O compound. The Fourier transforms of the calculated spectra are compared with the experimental one and shown in figure 5(a). The disagreement between the Fourier transform of Cu_2O and the other Fourier transforms indicates that the SEELFS and SEXAFS techniques have the capacity to distinguish the different local structures (see also figure 5(b)). The Fourier transform of the missing-row model gives a much better agreement with the experimental one than that of the buckled model. Therefore we conclude that the missing-row model is a more rational model for the (2×1) structure than the buckled model. The first maximum of the curved-wave Fourier transform agrees well with the experimental one while the agreement with the second maximum is fairly good. The disagreement of the maxima at large distance may be caused by the neglect of the multiple scattering processes [30], by the possible deviation from the (2×1) structure and by the limitation of the resolution of the energy analyser.

We turn now to the O/Cu(111) system. The LEED investigations on the O/Cu(111) system showed that at room temperature only a disordered adsorption of oxygen atoms takes place [39]. This may be a reason for the fact that the O/Cu(111) system is less stable during the measurement than the O/Cu(110) system.

From the intensity of the Cu Auger peak at $E = 920$ eV and of the O Auger peak at $E = 510$ eV, the oxygen coverage can be determined [41]. In the case of 1200 L O exposure, the coverage is 0.35 monolayers.

From HREELS [7, 42] measurements, the oxygen adsorption in threefold sites was concluded. We assume that they are situated about 0.5 Å above the first copper layer (see the inset model in figure 5(b)). The first three copper neighbours ($R_1 = 1.91$, $R_2 = R_3 = 2.98$ Å) and the first oxygen neighbour were used for the calculation of the SEELFS spectrum. The Fourier transforms of the calculated and of measured SEELFS spectra show an excellent agreement for these neighbour distances (figure 5(b)).

It is determined from the SEELFS measurement that there exist three atoms at $R_1 = 1.91$ Å and together 6 neighbour atoms at $R_2 = R_3 = 2.98$ Å. This neighbour relation can be obtained if the oxygen atom is located about 0.5 Å above the topmost Cu atomlayer and the three nearest copper atoms shift about 0.3 Å laterally. This result coincides with the LEIS (low energy ion scattering) result [43] which indicates a displacement of the Cu atoms of 0.3 Å and the SEXAFS result [7].

4. Conclusion

The plane-wave phaseshift for the Cu-O nearest-neighbour distance deviates from both the reference phaseshift and from the curved-wave phaseshift, as can be seen from figure

3. The apparent shorter nearest-neighbour distance [11, 12] is therefore caused by the use of the plane-wave phaseshift. In addition, the total phaseshift depends now on the distance (cf equations (2) and (3)). The total phaseshift for $R = 3.1 \text{ \AA}$ differs clearly from that for $R = 2.0 \text{ \AA}$ (see figure 3). Thus the reference phaseshift can only be used when the neighbour distance does not deviate clearly from that of the reference system. The reference phaseshift of the nearest-neighbour distance cannot be applied to further neighbour shells. By using the curved-wave approximation, all neighbour distances can be correctly determined, provided the quality of the spectrum and the surface is good enough. According to LEED studies [39], the Cu(110) surface shows a (2×1) substructure after 60–600 L oxygen exposure. There are many studies available where the location of oxygen atoms and the reconstruction of the Cu atoms of this surface was investigated [5, 6, 9, 44, 45]. Our results (the missing-row model and $R_1 = 1.82 \text{ \AA}$) are in good agreement with the SEXAFS results of Döbler *et al* [9, 46]. The oxygen atoms are located slightly above the first Cu layer (0.3 \AA). The broadening of the first peak of the experimental Fourier transform (see figure 5(a)) is caused by two different neighbour distances. Indeed, the first maximum involves two neighbour distances (R_1 and R_2 of the inset model in figure 5(a)).

Acknowledgments

We thank Prof Dr E Zeitler for his continued interest. One of us, BL thanks the Max-Planck-Gesellschaft for financial support.

References

- [1] Stöhr J, Denley D and Perfetti P 1978 *Phys. Rev. B* **18** 4132
- [2] Stern E A, Sayers D E, Shechter J G and Bunker B 1977 *Phys. Rev. Lett.* **38** 767
- [3] Hodgson K O, Hedman B and Penner-Hahn J E (ed) 1984 *EXAFS and Near Edge Structure III* (Berlin: Springer)
- [4] Stöhr J 1985 *X-Ray Absorption: Principles, Applications, Techniques of EXAFS, SEXAFS and XANES* ed R Prins and D Königsberg (New York: Wiley) p 443
- [5] Döbler U, Baberschke K, Haase J and Puschmann A 1984 *Phys. Rev. Lett.* **52** 1437
- [6] Haase J 1988 *Physics of Solid Surfaces* vol 36, ed J Koukal (Amsterdam: Elsevier) p 37
- [7] Haase J and Kuhr H J 1988 *Surf. Sci.* **203** L695
- [8] Puschmann A, Haase J, Crapper M D, Riley C E and Woodruff D P 1985 *Phys. Rev. Lett.* **54** 2250
- [9] Bader M, Puschmann A, Ocal C and Haase J 1986 *Phys. Rev. Lett.* **57** 3273
- [10] Döbler U, Baberschke K, Stöhr J and Outka D A 1985 *Phys. Rev. B* **31** 2532
- [11] Stöhr J 1978 *Japan. J. Appl. Phys.* **17-2** 217
- [12] Hillert B and Haase J private communication
- [13] De Crescenzi M 1982 *EXAFS and Near Edge Structure* ed A Bianconi, L Incoccia and S Stipcich (Berlin: Springer) p 382
- [14] Hitchcock A P and Teng C H 1985 *Surf. Sci.* **149** 558
- [15] Santoni A and Urban J 1987 *Solid State Commun.* **63** 257
- [16] Santoni A, Tran Thoai D B and Urban J 1986 *Solid State Commun.* **58** 315
- [17] De Crescenzi M, Papagno L, Chiarello G, Scarmozzino R, Colavita E, Rosei R and Mobilio S 1981 *Solid State Commun.* **40** 613
- [18] Tran Thoai D B and Ekaradt W 1990 *Solid State Commun.* **75** 143–6
- [19] Luo B and Urban J 1990 *Surf. Sci.* **239** 235–42
- [20] Santoni A and Urban J 1987 *Surf. Sci.* **186** 376
- [21] Della Valle F, Comelli G, Zanini F, Rosei R and Paolucci G 1988 *Phys. Rev. B* **38** 13355
- [22] De Crescenzi M, Antonangeli F, Bellini C and Rosei R 1983 *Phys. Rev. Lett.* **50** 1942

- [23] De Crescenzi M, Chiarello G, Colavita E and Rosei R 1982 *Solid State Commun.* **44** 845
- [24] Tyliszczak T, Esposito F and Hitchcock A P 1989 *Phys. Rev. Lett.* **62** 2551
- [25] Müller J E and Schaich W L 1983 *Phys. Rev. B* **27** 6489
- [26] McKale A G, Knapp G S and Chan S-K 1986 *Phys. Rev. B* **33** 841
- [27] Rehr J J, Albers R C, Natoni C R and Stern E A 1986 *Phys. Rev. B* **34** 4350
- [28] Bethe H 1933 *Handbuch der Physik, Quantentheorie* (Berlin: Springer)
- [29] Santoni A *PhD Thesis* FU Berlin
- [30] Lee P A, Citrin P H, Eisenberger P and Kincaid B M 1981 *Rev. Mod. Phys.* **53** 769
- [31] Naas J 1961 *Mathematisches Wörterbuch* (Berlin: Akademie)
- [32] Edmonds A R 1957 *Angular Momentum in Quantum Mechanics* (Princeton, NJ: Princeton University Press)
- [33] Herman F and Skillman S 1963 *Atomic Structure Calculation* (Englewood Cliffs, NJ: Prentice-Hall)
- [34] Teo B K and Lee P A 1979 *J. Am. Chem. Soc.* **101** 2815
- [35] Manson S T 1972 *Phys. Rev. A* **6** 1013
- [36] Leapman R D, Rez P and Mayers D F 1980 *J. Chem. Phys.* **72** 1232
- [37] Manson S T and Cooper J W 1968 *Phys. Rev.* **165** 126
- [38] Luo B and Urban J 1990 *Solid State Commun.* at press
- [39] Ertl G 1967 *Surf. Sci.* **6** 208
- [40] Habkraken F H P M and Bootsma G A 1979 *Surf. Sci.* **87** 333
- [41] Habkraken F H P M, Kiefer E Ph and Bootsma G A 1979 *Surf. Sci.* **83** 45
- [42] Dubois L H 1982 *Surf. Sci.* **119** 399
- [43] Niehus H 1983 *Surf. Sci.* **130** 41
- [44] De Wit A G J, Bronckers R P N and Fluit J M 1979 *Surf. Sci.* **82** 177
- [45] Feidenhans'l R and Stensgaard I 1983 *Surf. Sci.* **133** 453
- [46] Haase J, Hillert B and Bradshaw A M 1990 *Phys. Rev. Lett.* **64** 3098